Theoretical Analysis of Heat Flow and Structural Changes during Laser Transformation Hardening of Hypo-Eutectoid Steel †

Katsunori INOUE*, Etsuji OHMURA**, Koichi HARUTA*** and Shoichi IKUTA***

Abstract

The present paper deals with the heat flow and solid-state phase transformations during the laser transformation hardening of hypo-eutectoid steel. A finite-difference computer model was developed to analyze the changes with time of heat flow, the carbon redistribution in austenite and the subsequent quenching to martensite during laser transformation hardening. The analyzed results were shown in the pseudo-color images on the display. Furthermore, experimental surface transformation hardening was carried out using a square beam of uniform energy distribution, and the results were in good agreement with the theoretical results obtained by the computer model. The transformation hardening process can be also simulated for any given hypo-eutectoid steel under any laser irradiating condition. The computer model proposed in the present paper can be applied to determine theoretically the best combination of the process variables for the laser transformation hardening in advance.

KEY WORDS: (Laser Materials Processing) (Laser Transformation Hardening) (CO_2 Laser) (Finite Difference Method) (Hypo-eutectoid Steel) (Heat Conduction) (Phase Transformation) (Microstructure) (Computer Simulation)

1. Introduction

Due to the recent development of high power, continuous wave CO_2 lasers, the laser transformation hardening has drawn a great deal of attention. The final product obtained by the laser transformation hardening depends complicatedly on the process variables. These variables are summarized as the following two factors. One is the laser irradiating conditions, that is, the power, size and shape of the laser beam, and the traveling velocity. The other is the work material, that is, the chemistry and metallurgy of the steel. In the industrial use of the laser transformation hardening, it is important to determine the best combination of the process variables for a given application and for a given steel. It is the purpose of this study to develop a computer simulation system which enables to determine theoretically the best combination of the process variables in advance.

In this paper, a finite-difference computer model is developed to analyze theoretically the heat flow, the transformation of pearlite and ferrite to austenite, and its subsequent quenching to martensite, so as to predict the microstructure and the hardness in the heat-affected zone during laser transformation hardening. The analyzed results are shown in the pseudo-color images on the display. Furthermore, experimental laser transformation hardening is carried out, and the results are compared with the theoretical results obtained by the computer model.

2. Analysis of Heat Flow

Shown in **Fig. 1** is a sketch[1] of the transformation hardening process with laser irradiation. The laser beam is stationary while the workpiece moves at a constant velocity v in the x direction. Except during the initial and the final transients of the laser transformation hardening process, the temperature distribution in a workpiece of sufficient length is steady with respect to both the coordinate system and the heat source. Under such conditions, the process is reduced to a steady state heat flow problem. The Fourier equation for a stationary coordinate system is given as

† Received on Nov. 4, 1987
* Professor
** Research Instructor
*** Graduate Student of Osaka University

Transactions of JWRI is published by Welding Research Institute of Osaka University, Ibaraki, Osaka 567, Japan

$$\nabla \cdot (\lambda \nabla T) - v \frac{\partial (c\rho T)}{\partial x} = 0, \tag{1}$$

where T is temperature, c specific heat, ρ the density and λ the thermal conductivity of the workpiece material. We analyze the temperature distribution which is symmetric with respect to the x-z plane.

In order to consider the temperature dependence of the thermophysical properties, the finite difference equations are derived using the implicit Crank-Nicolson method. **Figure 2** shows the grid system for calculation of the heat flow. Considering that the temperature varies violently near the heat source and slowly at the other area, the logarithmic grid is employed in y and z direction. The uniform grid is employed in x direction in order to calculate the temperature distribution in detail at the area where the structural changes are to be analyzed (see Fig. 1). The finite difference equation for the point (i, j, k) is

$$\begin{aligned} T_{i,j,k} = \frac{1}{F_{i,j,k}} (&F_{i+1}\, T_{i+1,j,k} + F_{i-1,j,k}\, T_{i-1,j,k} \\ &+ F_{j+1}\, T_{i,j+1,k} + F_{j-1}\, T_{i,j-1,k} \\ &+ F_{k+1}\, T_{i,j,k+1} + F_{k-1}\, T_{i,j,k-1}), \end{aligned} \tag{2}$$

where $T_{i,j,k}$ is the temperature at the point (i, j, k), and

$$F_{i\pm1} = \frac{2\lambda_{i,i\pm1} \mp (c\rho)_{i\pm1,j,k} v \Delta x}{4(\Delta x)^2}, \tag{3}$$

$$F_{j+1} = \frac{\lambda_{j,j+1}}{\Delta y_j (\Delta y_j + \Delta y_{j-1})}, \tag{4}$$

$$F_{j-1} = \frac{\lambda_{j,j-1}}{\Delta y_{j-1} (\Delta y_j + \Delta y_{j-1})}, \tag{5}$$

$$F_{k+1} = \frac{\lambda_{k,k+1}}{\Delta z_k (\Delta z_k + \Delta z_{k-1})}, \tag{6}$$

$$F_{k-1} = \frac{\lambda_{k,k-1}}{\Delta z_{k-1} (\Delta z_k + \Delta z_{k-1})}, \tag{7}$$

$$\begin{aligned} F_{i,j,k} = &F_{i+1} + F_{i-1} + F_{j+1} \\ &+ F_{j-1} + F_{k+1} + F_{k-1}, \end{aligned} \tag{8}$$

where $\lambda_{i,i\pm1}$ and the like are the mean values of thermal conductivity between two grid points and are given as follows[2]:

$$\lambda_{i,i\pm1} = \frac{2\lambda_{i,j,k}\lambda_{i\pm1,j,k}}{\lambda_{i,j,k} + \lambda_{i\pm1,j,k}}, \tag{9}$$

$$\lambda_{j,j\pm1} = \frac{2\lambda_{i,j,k}\lambda_{i,j\pm1,k}}{\lambda_{i,j,k} + \lambda_{i,j\pm1,k}}, \tag{10}$$

$$\lambda_{k,k\pm1} = \frac{2\lambda_{i,j,k}\lambda_{i,j,k\pm1}}{\lambda_{i,j,k} + \lambda_{i,j,k\pm1}}, \tag{11}$$

At the top surface of the workpiece, $2w_{i,j}/[\Delta x (\Delta y_{j-1} + \Delta y_j) \Delta z_0]$ is added in the parenthesis of the right side of the finite difference equation which corresponds to Eq. (2), where $w_{i,j}$ is the heat input to the $(i, j, 0)$ grid. If the absorptivity ϵ is uniform at the top surface, the sum total of $w_{i,j}$ is equal to ϵP, where P is the incident laser power.

Kou et al[3] have shown through numerical calculations that the influence of the surface heat loss caused by convection or thermal radiation on the temperature distribution in the workpiece during laser transformation hard-

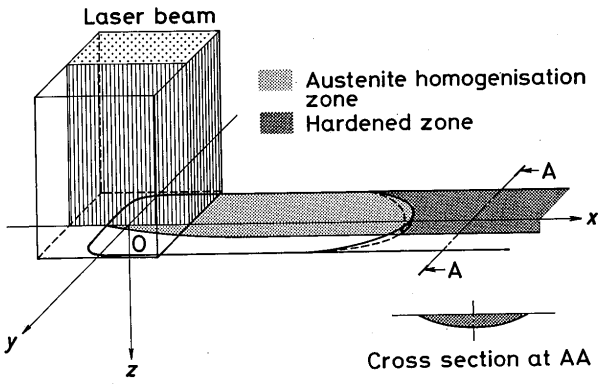

Fig. 1 A schematic sketch of the transformation hardening process with laser irradiation.

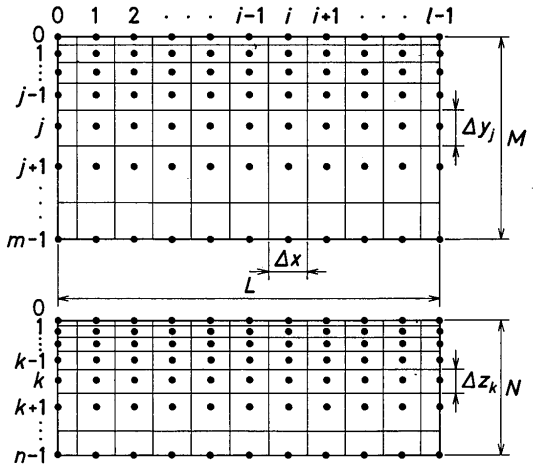

Fig. 2 Grid system for calculation of heat flow.

ening is negligibly small. Therefore, these surface heat losses are ignored in this study. This assumption will be discussed again later on. The heat of solid-state transformations is usually very small and, therefore, is ignored in the calculation.

3. Analysis of Structural Changes by Heat Cycle

3.1 Formation of austenite from pearlite

The pearlite colonies are transformed to austenite above A_{C1} point on heating. **Figure 3**[4] illustrates the two-dimensional model which is used to determine the carbon diffusion from a layer of cementite into an adjacent layer of ferrite. Fick's Laws permit the concentration of carbon to be determined as a function of distance and time.

Figure 4[4] shows the dissolving distance of cementite, which corresponds to the position B in Fig. 3, in a standard pearlite colony of eutectoid steel with time elapsed after the cementite starts to dissolve at various heating rate. The average spacing of lamellae and the average diameter of pearlite colonies is assumed to be 480nm and 80μm. The calculation was carried out using the alternating direction implicit (ADI) method, in which temperature dependence[5] of the diffusion coefficient of carbon was considered. It is clear that the time required for the pearlite to be transformed to austenite becomes shorter as the heating rate increases. When the heating rate is 10^5K per second, the pearlite dissolution requires about 3ms at most. These results show the pearlite is transformed almost instantaneously to austenite, when a hypo-eutectoid steel is heated above the A_{C1} point during laser transformation hardening.

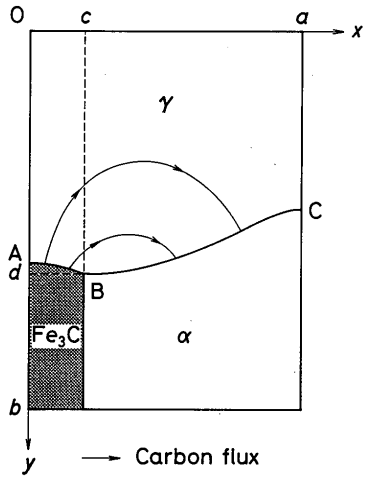

Fig. 3 Diffusion geometry for dissolution of pearlite.

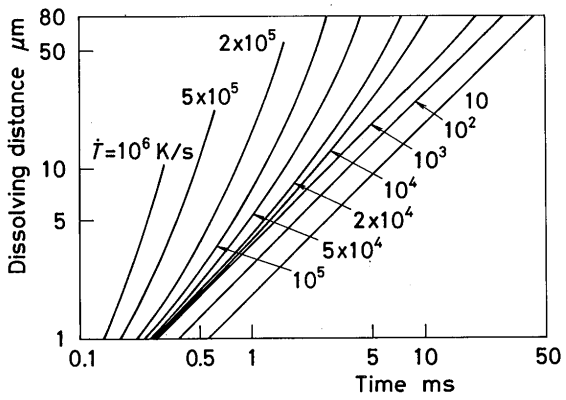

Fig. 4 Dissolving distance d in Fig. 3 with time at various heating rate.

3.2 Homogenisation of austenite

The carbon redistribution in austenite during laser transformation hardening, where the carbon diffuses from the high to the low concentration regions, depends on temperature and time. The heat-affected-zone microstructure with laser irradiation varies remarkably in z direction as will be shown later. It can be regarded that the redistribution occurs in the y-z plane, mainly. Then the differential equation of carbon diffusion is:

$$\frac{\partial C}{\partial t} = \nabla \cdot (D \nabla C) \tag{12}$$

where C is the carbon concentration in austenite, and D is the diffusion coefficient of carbon in austenite.

In order to consider the temperaure dependence of the diffusion coefficient of carbon, the finite difference equations are derived using the ADI method. **Figure 5** shows

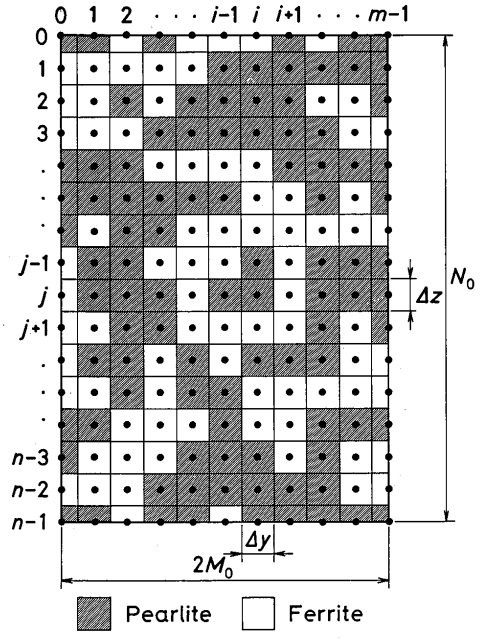

Fig. 5 Grid system for calculation of carbon redistribution in austenite.

the grid system used, where the uniform grid is employed. The laser beam is traveling perpendicularly to the grid system. In this study, the initial structure of workpiece, which is composed of ferrite and pearlite, is input to an image processor through a microscope and a TV camera, then the information of two-valued image, which corresponds to Fig. 5, is transfered to a computer for numerical calculations.

The computational progress is as follows. First, the temperature is determined as a function of position and time through the heat flow calculation in Section 2. This result of temperature is used to determine the momentary value of diffusion coefficient of carbon at each grid. Then the carbon redistribution process in austenite is computed at the area where the temperature rises above A_{c1} point.

3.3 Martensitic transformation

On subsequent cooling, austenite is transformed to martensite or fine-pearlite, if the cooling rate is higher than the critical cooling rate or not, respectively. The critical cooling rate depends on the carbon concentration as shown in **Fig. 6**[6]. The temperature at which austenite starts to be transformed to martensite, that is, M_S point depends on the composite of the austenite and is given as[7],

$$M_S\,(K) = 811 - 317C - 33Mn - 28Cr - 17Ni - 11Si - 11Mo - 11W. \quad (13)$$

In this study, cooling rate at each grid in Fig. 5 is calculated at 973K {700°C} using the calculated results of the heat flow in Section 2. The M_S point at each grid is also determined by Eq. (13), considering the carbon concentration at the grid mesh.

4. Laser Transformation Hardening Experiments

4.1 Experimental Procedures

The transformation hardening was carried out using a continuous wave CO_2 laser developed GTE SYLVANIA Co. The maxmum power capacity was 5kW. An integration mirror and a Zn-Se lense were used to generate a square laser beam of uniform energy distribution[8].

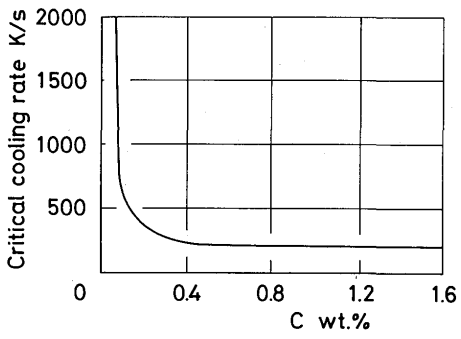

Fig. 6 Critical cooling rate of carbon steel.

The laser irradiating condition is shown in **Table 1**. The workpiece was 120mm long, 50mm wide, and 15mm thick, and the work material is rolled carbon steel S45C which is equivalent to AISI 1045. The chemical composition of the material used is shown in **Table 2**.

The top surface of the workpiece was machined smooth, and coated with carbon 60μm thick in order to enhance the surface absorptivity. Ohmura et al[9] have shown experimentally and theoretically that there is the optimum thickness of coated film to improve the absorption of the CO_2 laser beam.

After the laser irradiation, the workpiece was sectioned transverse to the direction of travel, polished, and etched with 5 pct Nital. The microstructure of the heat-affected zone was examed by a metallographic microscope.

4.2 Heat-affected-zone microstructure

The microstructure of the heat affected zone is shown in **Fig. 7**. The present case depth is about 470μm. The middle of Fig. (e) is the boundary of the heat affected zone. Slightly above this boundary the pearlite colonies were transformed to austenite, and transformed to martensite on subsequent cooling. These pearlite colonies didn't have sufficient time to interact with their neighboring ferrite and, consequently, their carbon content remained essentially unchanged[10]. According to Ref. 11) pearlite starts transforming to austenite at about 1063K when the heating rate exceeds 200K per second or so. Since the heating rates involved in the present study, as will be shown later, are far greater than 200K per second, the boundary of the heat affected zone corresponds to a peak temperature of 1063K.

Further up into the heat affected zone, both the peak temperature and diffusion time increased. As a result, the prior-pearlite colonies expanded while being austenitized and formed martensite colonies of lower carbon content[10] during subsequent cooling, as can be seen at Position (c) and (d). The rings surrounding these martensite

Table 1 Laser irradiating condition.

Laser power	1.11 kw
Beam size	4.5 mm x 4.5 mm
Traveling velocity	30 mm/s

Table 2 Chemical somposition of material used.

C	Si	Mn	P	S	Cu	Ni	Cr
0.46	0.22	0.81	0.016	0.009	0.01	0.02	0.02

(wt. %)

colonies or ferrite are fine pearlite[10]. The remaining ferrite phase is unaffected by the diffusion of carbon atoms. The ferrite grain size here is significantly smaller than that of the base metal.

At the top of the heat affected zone, as shown in Fig. 7 (b), there is no ferrite, and the martensite colonies are of lower carbon contents than those at Position (c), due to further increase in the peak temperature and the diffusion time.

5. Analytical Results and Discussion

In this study, a mini-computer, HITAC E-800, was used to carry out the calculations of the heat flow, the carbon redistribution in the austenite and subsequent quenching to martensite. The analytical results on the structural changes by the heat cycle are shown in the pseudo-color images on the display.

Figure 8 shows the temperature distribution in the workpiece during transformation hardening under the laser irradiating condition shown in Table 1. The successive over-relaxation (SOR) method (with a relaxation parameter of 1.25) was employed to solve the finite difference equations which are composed of Eq. (2) and so on. The size of L, M and N in Fig. 2 was set at 16.5mm, 7mm and 5mm respectively, and the grid points were given by $l = 110$, $m = 20$ and $n = 18$. The initial temperature was given to be 293K. The absorptivity was assumed to be constant in the heat flow calculation. By using 1063K as the effective A_{C1} temperature on heating and considering the temperature dependence of the thermophysical properties of S45C carbon steel[2], the size of the heat affected zone was calculated. An absorptivity of 72.7 pct was found to fit best both the depth and the width of the heat affected zone observed.

The broken lines in Fig. 8(a) show the shape of the heat source. The maximum temperature at the workpiece surface is near the end edge, rather than at the center, of the rectangular heat source. The cooling rate is relatively greater than the heating rate. There is much difference in the heat cycle between the rectangular heat source and the Gaussian heat source[1]. The time scale in this figure is used to show the structural changes, as will be shown later, where time zero corresponds to the edge of the finite difference model to calculate the heat flow (see Fig. 2).

The surface heat loss due to radiation from the calculated area of O-xy plane, q_r, is evaluated as about 4.7W, assuming that the emissivity of the surface is 1 and the surrounding temperature is 293K. The heat loss from the top surface of the workpiece due to forced convection[12] caused by traveling of the workpiece, q_c, is estimated

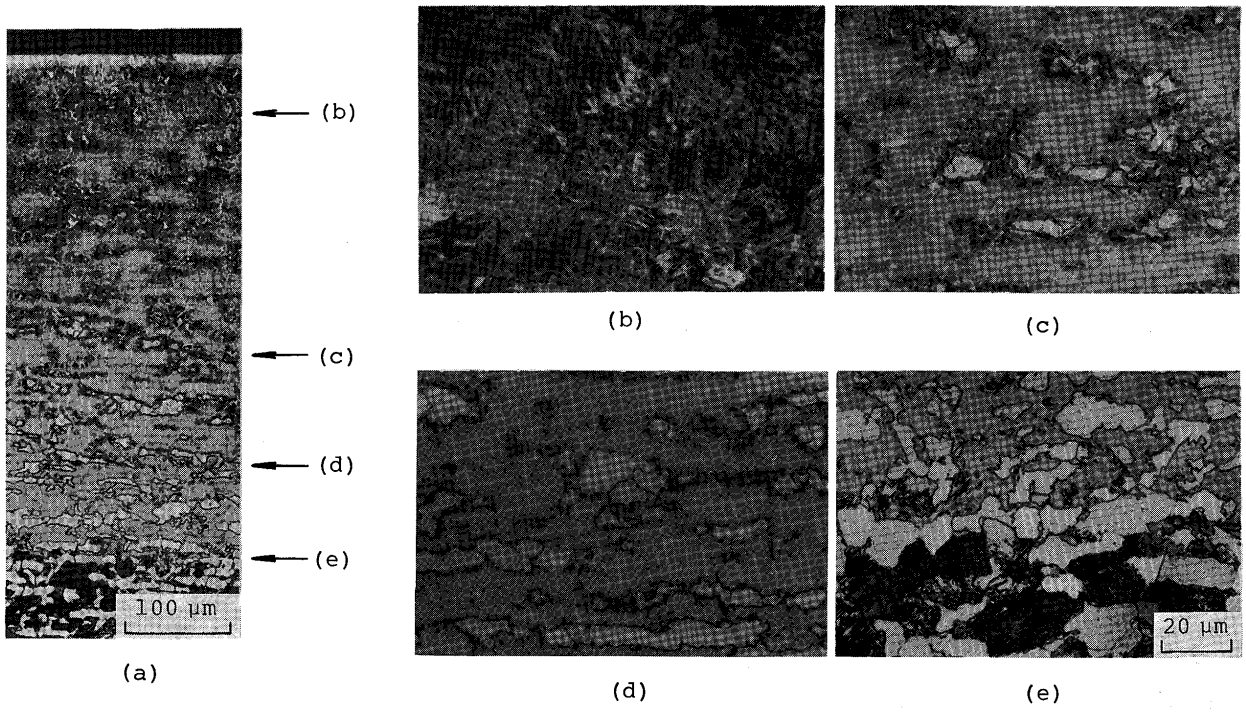

Fig. 7 Microstructure of the heat affected zone of S45C steel: (a) transverse cross-section; (b) to (e) higher magnification of (a). Magnification of (b) to (e) is same.

roughly at 15.4W, assuming that a plate which has the same length and width as the workpiece and whose top-surface temperature is 1700K is hold in parallel with a flow of air, whose temperature is 293K, with velocity 30mm/s. Therefore the total surface heat loss is about 20.1W and is 2.5 pct or so of the total amount of heat absorbed by the workpiece, which is overestimated, of cource, thus indicating that the heat loss from the workpiece surface is negligible as assumed in analysis of heat flow.

The analytical results of the structural changes calculated on the mini-computer with the heat cycle shown in Fig. 8 are expressed with the pseudo-color images on the CRT display through the workstation, ILANS, and the color image processor, NEXUS 6400, as shown in **Fig. 9**. The images with time are recorded by the video recorder and can be also expressed on the TV monitor as a sequential movable picture. The analytical results are expressed by twelve color codes, which depend on the carbon content and microstructure. The pearlite and ferrite are shown by white and black, respectively. The austenite and martensite are shown likes as land and sea in the map, respectively. The color codes are based on brown, yellow, green and blue, which correspond to the carbon concentration. The fine pearlite is shown by red in order to draw attention. Temperature and heating rate are also shown by two colored bands. The area size of structure used to analyze the structural changes is 240μm wide and 480μm deep, and the displayed structure in Fig. 9 is 160μm wide and 480μm deep. The carbon concentration of pearlite and ferrite is postulated to be 0.77wt.% and zero, respectively.

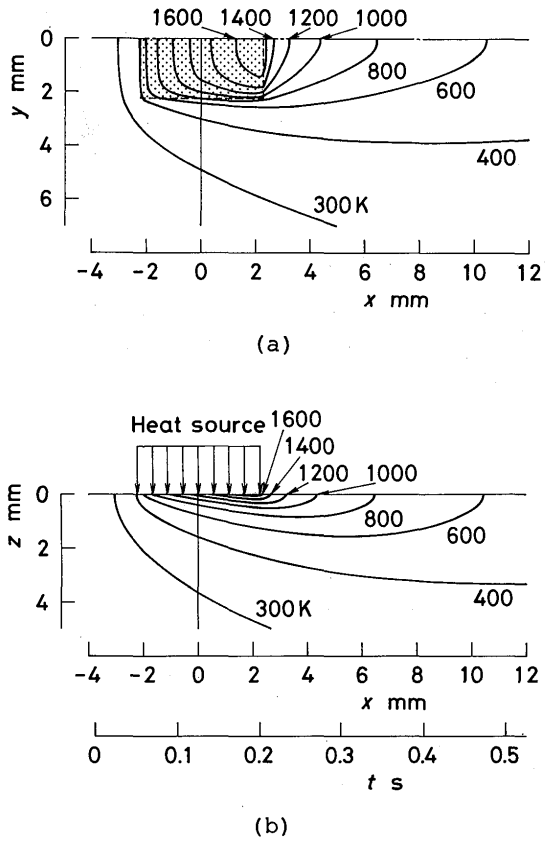

Fig. 8 Temperature distribution in the workpiece under the laser irradiating conditions shown in Table 1.

Figure 9(a) shows the structure when the front of the heat source has just reached. Any pearlite colony hasn't been transformed yet. The heating rate near the surface is about 2×10^4K per second. Figure 9(b) shows the state after the center of the laser beam has passed. The transformation of pearlite to austenite is progressing to the depth of about 280μm, and carbon has been already diffusing from the heigh to the low concentration regions near the top of the workpiece. Then the transformation of pearlite to austenite progresses more deeply untill the end edge of the square heat source reaches. Rapid self-quenching starts when the end edge of the laser beam has passed, as shown in Fig. 9(c). The cooling rate at the top of the workpiece is about 2.5×10^4K per second. The progress of the transformation of pearlite to austenite has almost stopped at the depth of about 470μm. The carbon redistribution in austenite is progressing pretty well and there is no ferrite near the surface.

In cooling period, the carbon atoms scarcely diffuse because the diffusion coefficient of carbon in austenite becomes small rapidly since the temperature decreases at high cooling rate. When the temperature decreases to the critical temperature, austenite of very low carbon concentration is transformed to fine pearlite first as a ring surrounding the higher carbon austenite, and then higher carbon austenite is transformed to martensite (Fig. 9(d)), because the M_s point becomes higher as the carbon concentration is lower. Still higher carbon austenite is being transformed gradually to martensite, as shown in Fig. 9(e), then almost all austenite is transformed to martensite at 0.55 second (Fig. 9(f)). Slightly above the boundary of the heat affected zone, the pearlite colonies are transformed to austenite without sufficient diffusion of carbon into the surrounding ferrite. Therefore, the carbon concentration of these martensite is almost 0.77 wt. pct, which is the same value as pearlite.

These analytical results are in good agreement with the experimental results shown in Section 4, thus indicating that the method of analysis proposed in this study is fully acceptable. The hardness of martensite depends on the carbon content, and martensite with a greater carbon parcentage has a higher hardness[10]. Therefore, these analytical results can be also used to estimate the hardness distribution in the heat affected zone. For any given

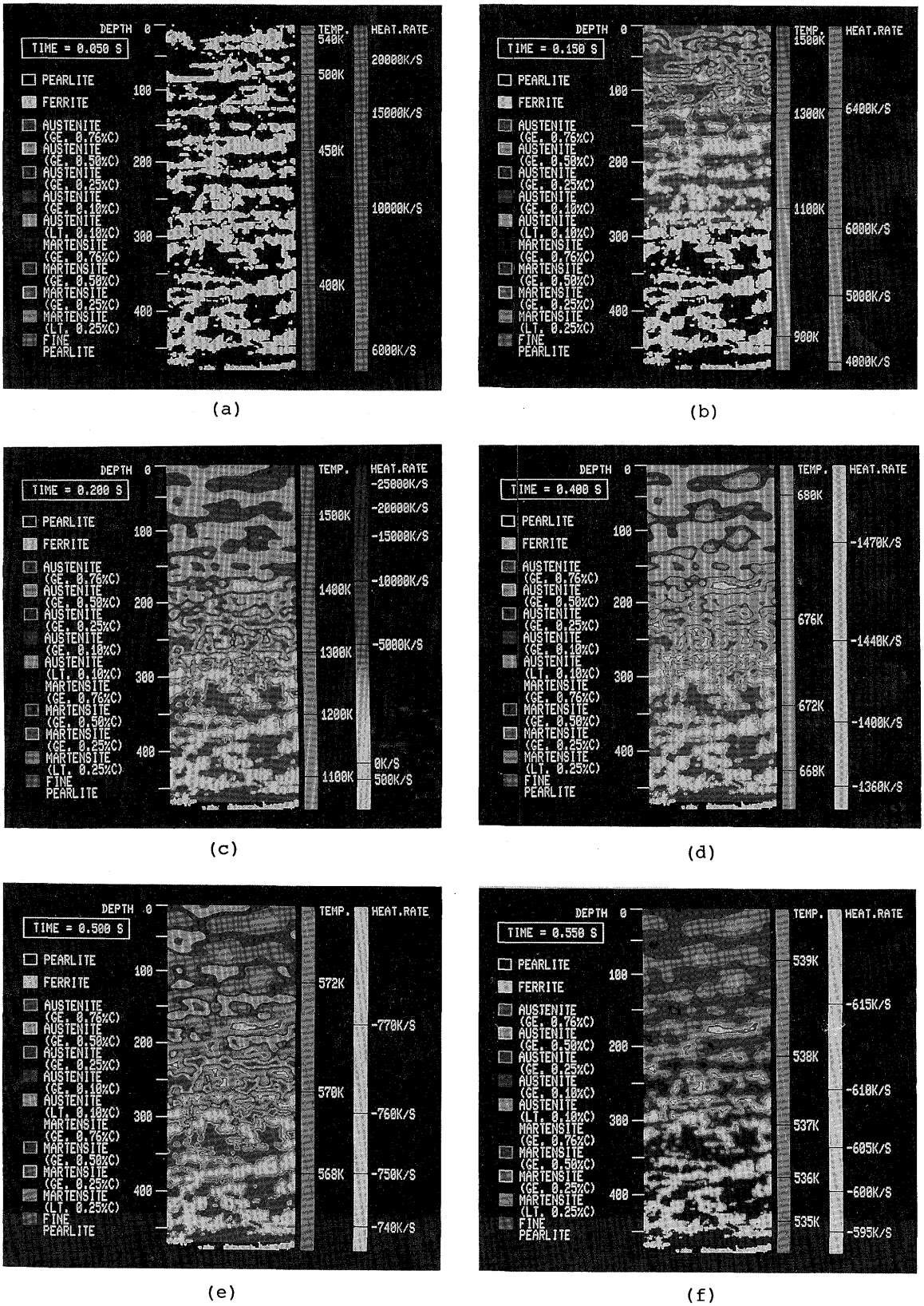

Fig. 9 Structural changes caused by the heat cycle shown in Fig. 8: (a) time 50ms; (b) time 150ms; (c) time 200ms; (d) time 400ms; (e) time 500ms; and (f) time 550ms.

hypo-eutectoid steel under any laser irradiaing condition, the transformation hardening process can be also analyzed. The present method of analysis can be applied to determine theoretically the best combination of the process variables for the laser transformation hardening in advance.

6. Conclusion

When the localized region on the surface of steel is irradiated by a high-powered laser beam for a short time, the cementite in the pearlite colonies in the vicinity of the area starts to dissolve at the A_{c1} point. Carbon atoms supplied from the dissolved cementite layer diffuse into the adjacent layer of ferrite and transform the ferrite to austenite. When the heating rate is 10^4K/s, the pearlite dissolution requires only about 10ms. As the pearlite colonies are transformed to austenite, carbon atoms diffuse into the ferrite which surrounds the pearlite colonies and transform the ferrite to austenite. As soon as the beam moves to another area of the surface, the austenite is self-quenched due to the heat conduction into the surrounding region of steel. Then the austenite starts the martensitic transformation at the M_S point which is determined by the carbon concentration of the austenite, if the cooling rate is heigher than the critical cooling rate. Because the M_S point becomes higher as the carbon concentration is lower, lower carbon austenite is transformed to martensite first, and then higher carbon austenite is transformed to martensite gradually. If the cooling rate is lower than the critical cooling rate, the low carbon austenite which surrounds the ferrite is transformed to the fine pearlite. The final structure and distribution of the carbon concentration of hypo-eutectoid steel under laser transformation hardening are determined after these process.

In this study, a finite-difference computer model is developed to analyze theoretically the above-mentioned structural changes on rapid heating and cooling during laser transformation hardening of hypo-eutectoid steel. The analytical results are shown in the pseudo-color images on the display. The computer model proposed in this study can be applied to determine theoretically the best combnation of the process variables for the laser transformation hardening in advance.

References

1) Namba, Y., Ohmura, E. and Makinouchi, S.: "A Study on Laser Hardening (2nd Rep., Analysis of Hardening Process)", *Trans. Japan Soc. Mech. Engrs.*, Ser. C, Vol. 50, No. 454, p. 1099 (1984–6) (in Japanese).

2) Ohmura, E., Namba, Y. and Makinouchi, S.: "Laser Hardening Using Step Functional Heat Input", *Bull. JSME,* Vol. 26, No. 219, p. 1670 (1939–9).

3) Kou, S., Sun, D.K. and Le, Y.P.: "A Fundamental Study of Laser Transformation Hardening", *Metallug. Trans.* A, Vol. 14A, No. 4, p. 643 (1983).

4) Inoue, K., Ohmura, E. and Ikuta, S.: "Computer Simulation on Transformation Process of Steel on Rapid Heating (Rep. I) –Formation of Austenite from Pearlite–", *Trans. JWRI,* Vol. 16, No. 1, p. 97 (1987).

5) Wells, C., Batz, W. and Mehl, R.F.: "Diffusion Coefficient of Carbon in Austenite", *Trans. AIME,* Vol. 188, p. 553 (1950).

6) Suzuki, H., *Saishin-Yousetsu-Handbook,* Sankaido, p. 227 (1977) (in Japanese).

7) *Kinzoku-Netsushori-Gijutsu-Binran,* Nikkan-Kogyo-Shinbunsha p. 25 (1961) (in Japanese).

8) Inoue, K., Ohmura, E., Gao, L.J. and Yi, N.: "Estimation of Interior Temperature Distribution of Work in Laser Materials Processing Using IR Camera (Rep. 1)", *Trans. JWRI,* Vol. 15, No. 1, p. 7 (1986).

9) Ohmura, E., Namba, Y., Makinouchi, S. and Sekimoto, Y.: "Temperature Distribution in a Two-Layer Disk Composed of a Metal and a Coated Film with Laser Irradiation", *Heat Transfer Japanese Research,* Vol. 14, No. 3, p. 32 (1985).

10) Ohmura, E. and Namba, Y.: "Microstructure of Hypo-Eutectoid Steel in Laser Hardening Process", *Trans. Japan Soc. Mech. Engrs.*, Ser. A, Vol. 51, No. 469, p. 2231 (1985) (in Japanese).

11) Orlich, J., Rose, A. and Wiest, P., *Atlas zur Wärmebehandlung der Sähle,* Verlag Stahleisen M.B.H., Vol. 3, p. 79 (1977).

12) *JSME Data Book*: *Heat Transfer,* 4th ed., p. 45 (1986) (in Japanese).